P4.3 TOWARD AN ERROR COVARIACE MATRIX OF RADAR RAINFALL ESTIMATES

Marc Berenguer(*), Isztar Zawadzki

J. S. Marshall Radar Observatory McGill University, Montreal, Quebec (Canada).

1. INTRODUCTION

Much effort has been put last years to assimilate radar observations (both reflectivity and radial velocity) into Numerical Weather Prediction (NWP) models (see, among others, Errico et al. 2000; MacPherson et al. 2003; Sun and Wilson 2003; Sun 2005). Moreover, as the model resolutions increase denser observations are required, and the resolution and coverage of the observations of radar networks make them very appropriate to be assimilated

However, the assimilation of radar observations has been implemented under a number of simplifying assumptions. For example, variational assimilation schemes explicitly require the error covariance matrix of the observations. In the case of radar measurements, their assimilation would require the characterization of their error covariance matrix. However, most of the existing schemes assume very simplifying hypotheses (namely, that these errors are homogeneous and not correlated).

The main purpose of the present study is to propose a physically based approach to deriving the error covariance matrix of radar rainfall estimates. Here, we do it for stratiform situations.

Recently, Germann et al. 2006 identified two main ways of characterizing the structure of the errors affecting radar rainfall estimates:

- Use an independent source of information as reference (such as rain gauges), and study the structure of the residuals between radar rainfall and the reference.
- Examine all relevant sources of error separately by simulation and/or experimental data analysis.

Here we opt for the second approach, which, besides characterization of the error covariance matrix of radar rainfall estimates, it allows us to better understand the physics and the role of the principal sources of errors, as well as their interactions, and in principle, to make the matrix adaptable to different meteorological situations.

2. FRAMEWORK OF THE STUDY

Due to the complexity of studying all the errors affecting radar rainfall estimates (see the reviews of Zawadzki 1984; Austin 1987; Joss and Waldvogel 1990), in this study we will focus on the two dominant sources of uncertainty in radar rainfall estimates at S-band:

- Range effects: which include the errors due to the increase of sampling volume and increase of the height of observations with range.
- The uncertainty associated to the transformation of radar reflectivity, Z, measurements into rain rate, R.

We analyze the structure of these two sources of error separately and examine the cross correlation between the two.

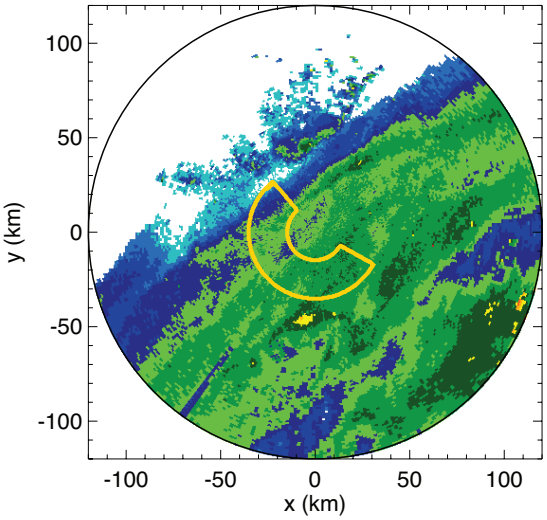

Fig. 1. 1.1 km-height CAPPI for 2333 UTC 16 September 1999. The yellow contour corresponds to the area from which observations have been used to simulate range-effects.

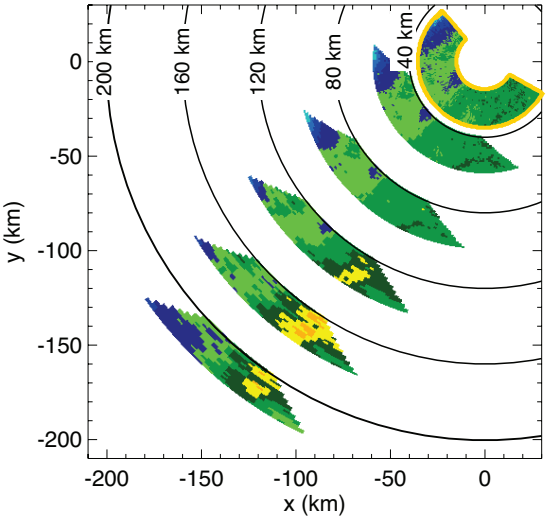

Fig. 2. Example of the 1.1 km-height CAPPI of the non-conformal simulations obtained for the real measurements observed in the selected near-range sector of reference (see figure 1).

3. RANGE EFFECTS

3.1 Data used

The data set we used to characterize the error due to range effects is that used by Bellon et al. 2005,

**Corresponding author address*: Marc Berenguer, Department of Atmospheric and Oceanic Sciences. McGill University. 805 Sherbrooke St. W. Montreal H3A2K6, Quebec (Canada).
Phone: (+1) 514 398 1849. email: berenguer@meteo.mcgill.ca

which consists of 287 hours of volumetric scans measured with the McGill S-band radar during 33 events of stratiform precipitation in Montreal, Quebec (Canada).

3D-reflectivity data over an area of 20 km by 200° close to the radar (yellow contour in figure 1) have been used to simulate radar measurements at further ranges by convolving real observations with the radar beam pattern (assumed Gaussianl -Doviak and Zrnic 1993-; more details of this simulation may be found in Bellon et al. 2005). Original observations (located at ranges between 15 and 35 km) have been considered to not be significantly affected by range effects and, thus, they have been used as the reference to which simulations at further ranges are be compared.

Figure 2 shows an example of the simulated observations generated for 5 sectors between 40 and 200 km every 40 km for the case presented in figure 1. The two main factors with range can be clearly observed: at further ranges, observations are obtained at higher elevations (the melting layer signature –the bright band- can be clearly appreciated in the simulations beyond 120 km) and the sampling volume becomes bigger.

In this framework, the error due to range effects is defined as:

$$\varepsilon_r(r,h) = dBZ^*(r,h) - dBZ(r_0,h_0) \qquad [1]$$

Where $dBZ^*(r,h)$ are the reflectivity simulations at range r and height h, and $dBZ(r_0,h_0)$ are the reflectivity observations at the reference height (1.1 km) in the reference sector shown in figure 1.

3.2 Characterization of the error

Bellon et al. 2005 have already quantified the mean error introduced by range effects and its variability. The mean error as a function of range and height of the observations for two particular range of bright band heights is shown in figure 3. This figure shows that the bias is kept within narrow limits below the bright band (BB); the BB introduces a severe overestimation of the reflectivity at ground; above the BB, the low returns of snow result in significant underestimation. The effect of the sampling volume can also be appreciated: bright band contamination extends higher up at further ranges where the beam is wider. The variability of the error (here quantified through its standard deviation) tends to increase with height, though more slowly as we go further in range due to the smoothing introduced in the observations by a wider beam.

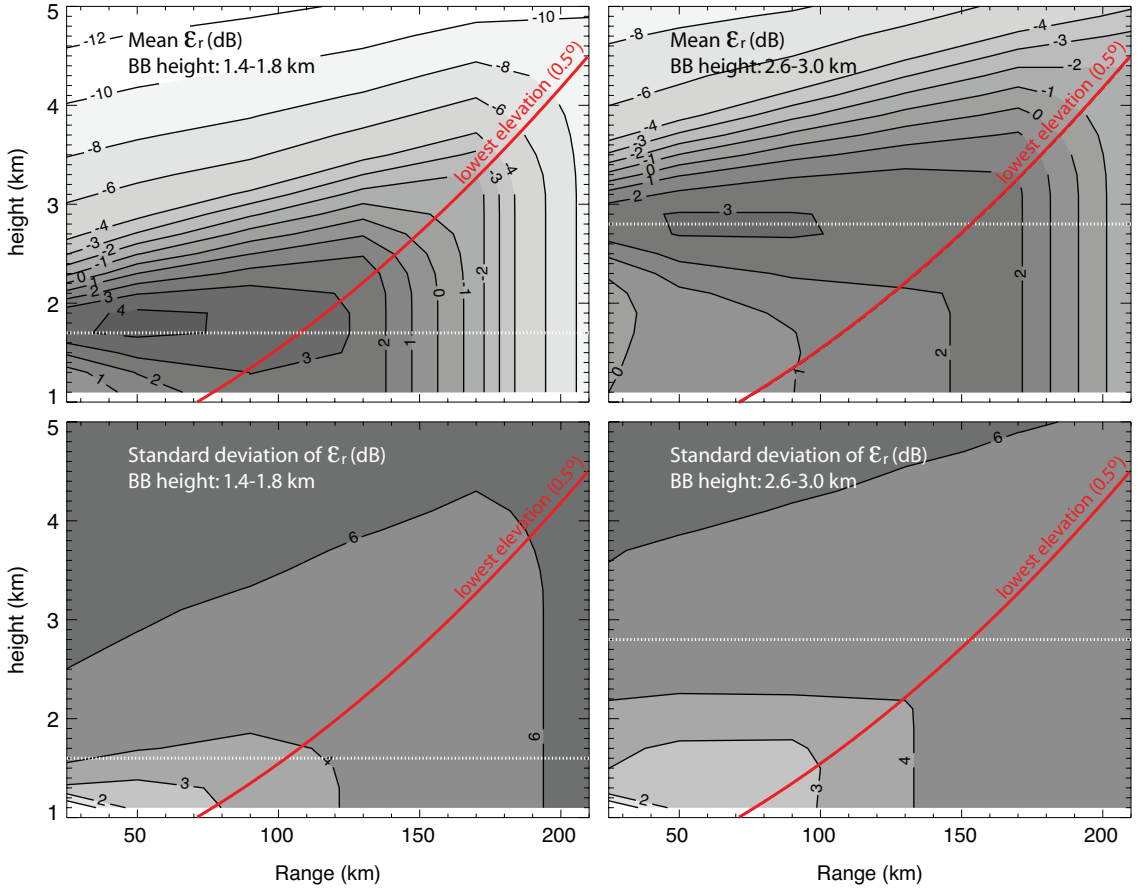

Fig. 3. Mean bias (top) and standard deviation (bottom) of the error due to range effects as a function of range and height of the measurements, when the bright band was between 1.4 and 1.8 km (left) and between 2.6 and 3.0 km (right). The red line corresponds to the path of the lowest elevation of the McGill S-band radar (0.5°) and the dotted line shows the mean height of the bright band for the analyzed scans.

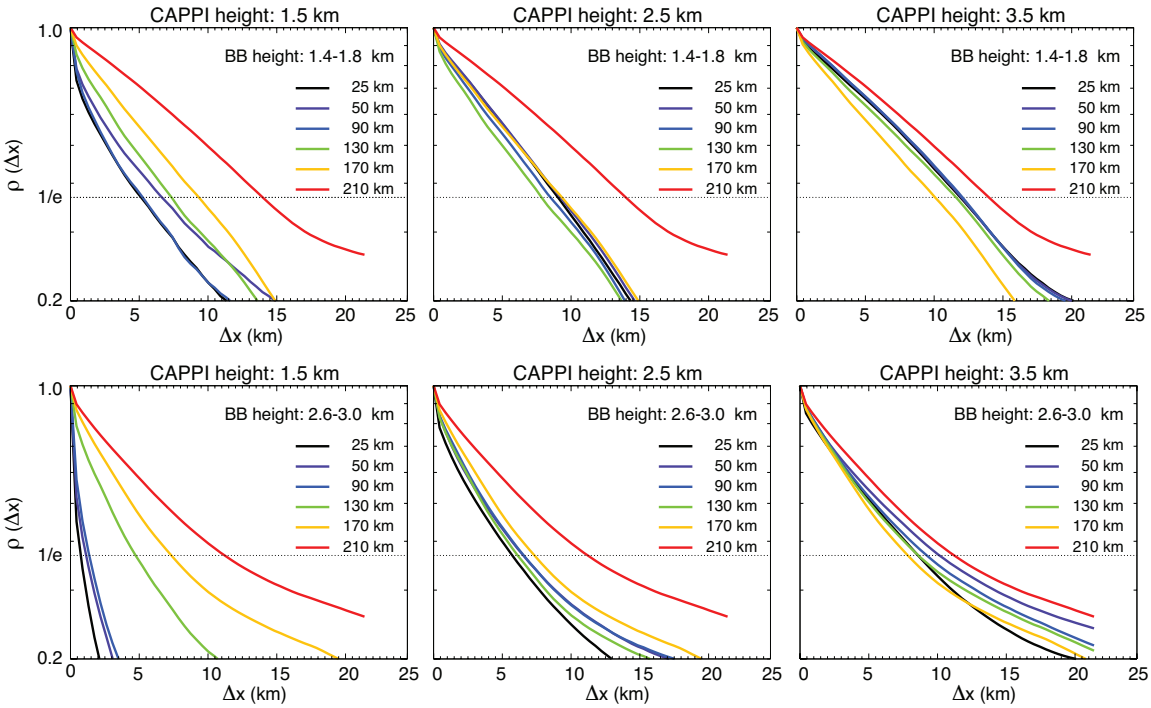

Fig. 4. ACFs corresponding to different CAPPI heights (from left to right, 1.5, 2.5 and 3.5 kms) for the cases with bright bands between 1.4 and 1.8 km (top) and between 2.6 and 3.0 km (bottom).

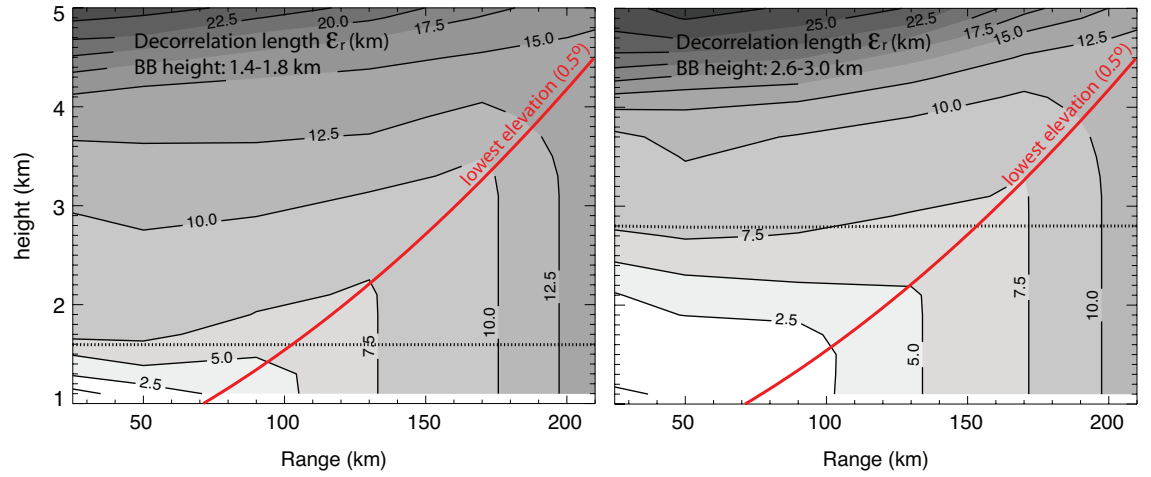

Fig. 5. Decorrelation distances of the error due to the range effects for the cases where the bright band is between 1.4 and 1.8 km (left) and between 2.6 and 3.0 km (right).

Furthermore, the same data set was used to compute the space autocorrelation functions (ACFs) of the errors introduced by the range effects (figure 4). It can be seen that the errors are almost uncorrelated when the radar measures in the liquid precipitation layer; they become more correlated in the melting layer (see also the decorrelation distances in figure 5) and the correlation is significantly higher in the snow region. On the other hand, the effect of beam broadening with range seems to have little influence in the space ACF of the errors due to range effects.

4. THE UNCERTAINTY IN THE Z-R RELATION

The uncertainty introduced by the Z-R transformation was studied by Lee and Zawadzki 2005 and Lee et al. 2007. In this section we will give a short review of their modeling methodology and their results for Montreal, Quebec (Canada).

Radar reflectivity is usually converted into rainfall rate using a power law such as:

$$Z = aR^b \tag{2}$$

Therefore, the error in rainfall from reflectivity observations can be expressed (in dB) as:

$$\delta R = 10\log\left[\left(\frac{Z}{a}\right)^{1/b}\right] - 10\log(R) \tag{3}$$

Figure 6 shows a *Z-R* scatter plot derived from DSD observations of a Precipitation Occurrence Sensing System (POSS -see a detailed description in

Sheppard 1990-) located in Montreal. The departures from the climatological model represent the uncertainty in rainfall estimated from reflectivity. The time evolution of δ_R is shown in figure 7 where it can be seen that the departures from a mean Z_R relationship exhibit significant structure in time (here, the decorrelation time is around 20-25 minutes –see figure 8a-). In particular, Lee et al. 2007 modeled the structure of δ_R through its Fourier spectrum as a power law (as shown in figure 8b).

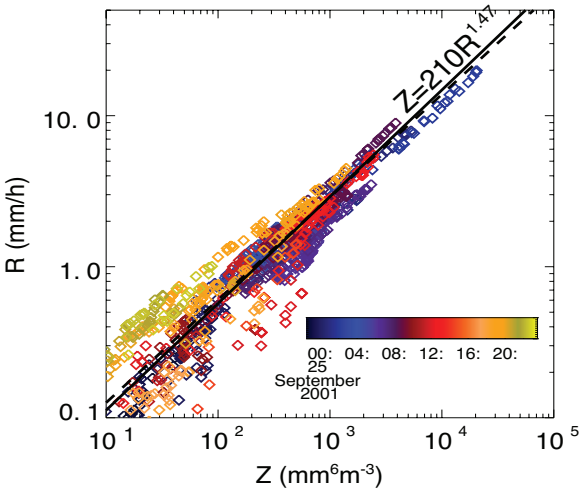

Fig. 6. Z-R scatterplot derived from POSS DSDs measured from 2135 UTC 24 September 2001 to 2335 UTC 25 September. The continuous line shows the best fitted power-law model for these observations and the dashed line shows the climatological Z-R relationship ($Z=200R^{1.47}$ -Lee and Zawadzki 2005-).

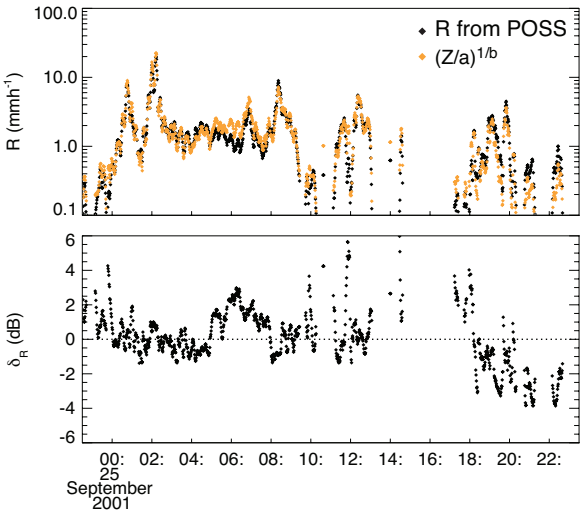

Fig. 7. Top: Series of rain rate (black dots) and of rain rate estimated from reflectivity using the climatological Z-R relationship (orange dots; both rain rate and reflecitivity obtained from POSS DSD observations). Bottom: residuals (in dB) between estimated and observed rain rate.

From a more climatological perspective and using a data set consisting of 60 days of DSD observations over 5 years with the same POSS, Lee and Zawadzki 2005 quantified the standard deviation of the error in radar rainfall estimates using a climatological Z-R relationship due to the uncertainty in the transformation, and they found it to be around 41%.

On the other hand, using the same data set, they found that the average decorrelation time of the residuals in this area is around 60 minutes. Assuming the Taylor hypothesis with the main speed of motion of storms for Montreal, this results in a mean decorrelation distance of around 40 km.

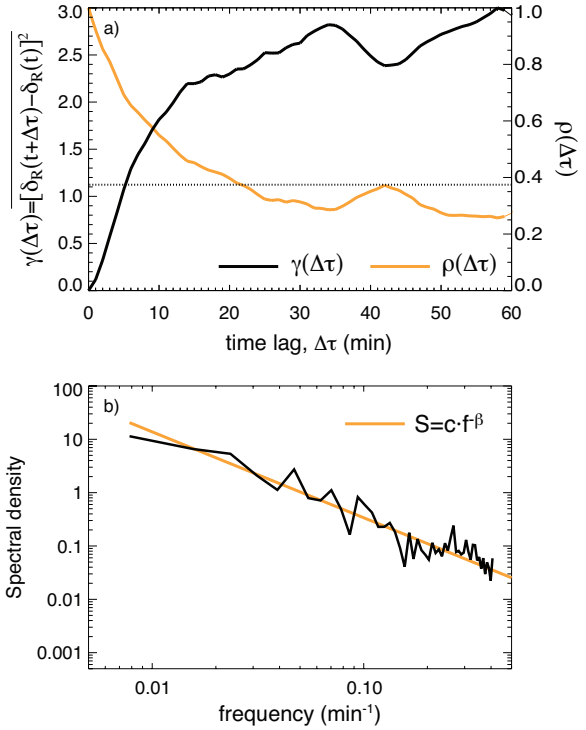

Fig. 8. Top: ACF and structure function of the time series of δ_R corresponding to the POSS observations of figures 6 and 7. Bottom: Fourier power spectrum of the same time series.

5. CORRELATION BETWEEN ERRORS

As mentioned in Section 2, besides evaluating the contribution of each source of error in the biases, variances and ACF of the resulting overall uncertainty, the crossed terms between errors should also be taken into account in order to fully characterize the error covariance matrix.

In this Section we will analyze the cross-correlation between the two analyzed sources of uncertainty for an individual event.

To do that, we have compared the series of δ_R obtained from DSDs measured with a POSS and the series of the error due to the vertical variation of reflectivity (i.e. the vertical profile of reflectivity –VPR- normalized by the reflectivity at a height of 1.1 km; figure 9d) derived from collocated profiles of reflectivity from data of the McGill S-band radar (see figure 9).

Figure 10 shows the cross correlation function of these two sources of error at different heights. It can be appreciated that the cross correlation in rain and snow regions is not significant, but that the correlation between the two errors increases and reaches the maximum (over 0.7) at the bright band height.

It is worth noting that this maximum appears for a time lag of 6 minutes, which, can be partly explained by the time drops need to fall to ground (considering that the bright band was around 3.5 km).

More analysis of this result and its possible implications for improving radar rainfall estimates can be found elsewhere in these Proceedings (Berenguer and Zawadzki 2007).

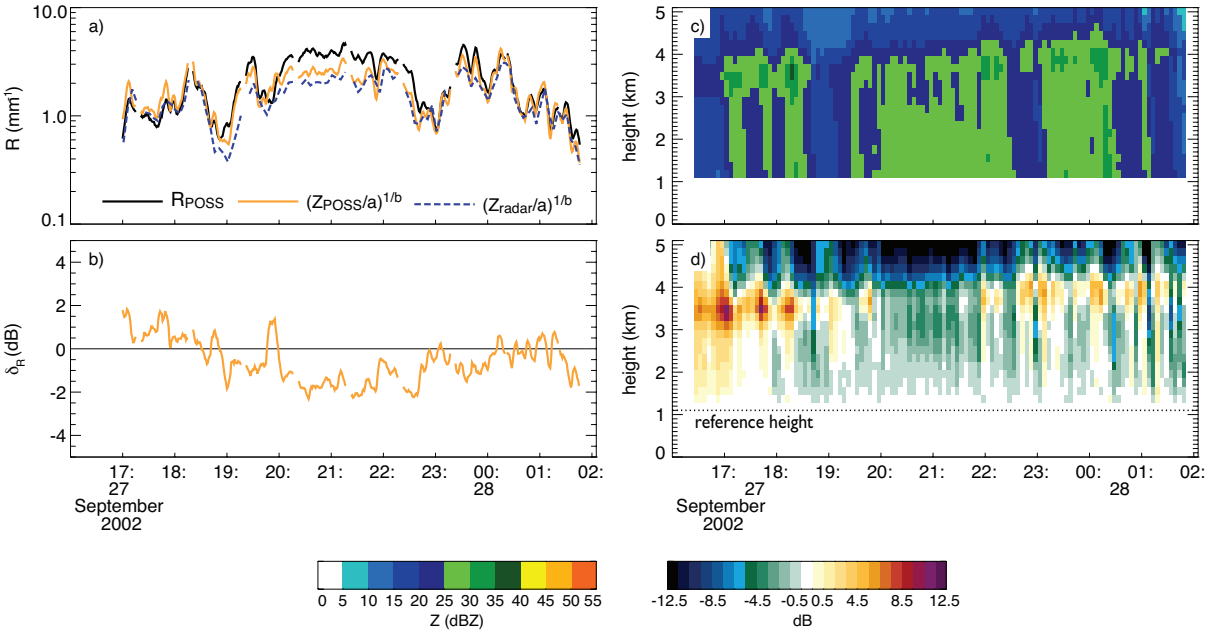

Fig. 9. (a) Comparison of the rain rate series corresponding to the event between 1600 UTC 27 September 2002 and 0200 UTC 228 September 2002 0200 UTC from POSS observations and estimated from POSS and radar reflectivity. (b) Series of δ_R from POSS observations. (c) Series of reflectivity profiles at POSS locatio0n observed with the McGill S-band radar.(d) Series of normalized VPRs obtained from radar observations.

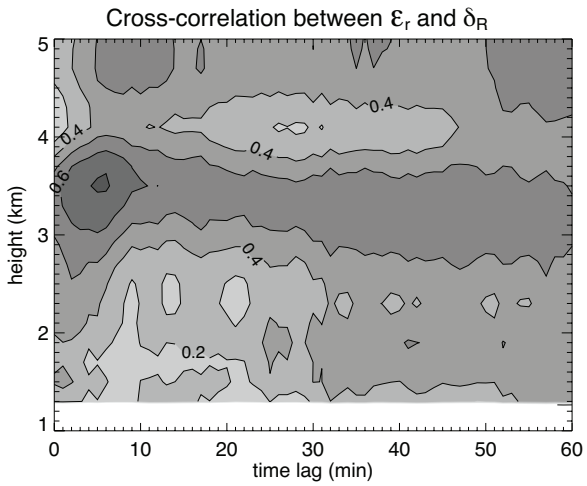

Fig. 10. Cross correlation between the residuals in R estimates due to the uncertainty in the Z-R transformation and the error due the range effects as a function of the height of radar measurements.

6. CONCLUSIONS

In the presented work we proposed a methodology to characterize the error covariance matrix of radar rainfall estimates in stratiform conditions with the purpose of their assimilation into NWP models.

The two main sources of error affecting S-band measurements (the errors due to range effects and the uncertainty due to the Z-R transformation) have been characterized separately from a physical perspective. A further stratification by storm types is possible.

In particular, the errors introduced by the range effects have been studied by simulation and it has been shown that they are more correlated in space when measurements are extrapolated from elevated observations (especially in the snow region, where the decorrelation distances can be up to 15-20 km). Thus, for models with grid spacing of ten kilometers and more the error covariance matrix due to this source of error can be considered diagonal. For higher resolution models the non-diagonal terms become important.

Stronger correlation has been found in the errors due to the Z-R transformation, which have been characterized from long-term DSD observations (the climatological decorrelation distance in Montreal has been found to be around 40 km).

Furthermore, we have also studied the correlation between the two sources of error analyzed. Significant correlation has been found between the extrapolation error from the melting layer and the residuals due to the Z-R transformation observed at ground.

References

Austin, P. M., 1987: Relation between Measured Radar Reflectivity and Surface Rainfall. Monthly Weather Review, 115, 1053-1070.

Bellon, A., G. Lee, and I. Zawadzki, 2005: Error statistics of VPR corrections in stratiform precipitation. Journal of Applied Meteorology, 44, 998-1015.

Berenguer, M. and I. Zawadzki, 2007: What does the bright band tell us about the Z-R relationship? Preprints, 33rd Conf. on Radar Meteorology, Cains, Australia, Amer. Meteor. Soc.

Doviak, R. J. and D. S. Zrnic, 1993: Doppler radar and weather observations. Dover Publications, INC, 562 pp.

Errico, R. M., L. Fillion, D. Nychka, and Z. Q. Lu, 2000: Some statistical considerations associated with the data assimilation of precipitation observations. Quarterly Journal of the Royal Meteorological Society, 126, 339-359.

Germann, U., M. Berenguer, D. Sempere-Torres, and G. Salvadè, 2006: Ensemble radar precipitation estimation - a new topic on the radar horizon. Preprints, Fourth European Conference on Radar in Meteorology and Hydrology, Barcelona, Spain, 559-562.

Joss, J. and A. Waldvogel, 1990: Precipitation measurement and hydrology. Radar in meteorology, D. Atlas, Ed., American Meteorological Society, 577-606.

Lee, G. W. and I. Zawadzki, 2005: Variability of drop size distributions: Time-scale dependence of the variability and its effects on rain estimation. Journal of Applied Meteorology, 44, 241-255.

Lee, G. W., A. W. Seed, and I. Zawadzki, 2007: Modeling the variability of drop size distributions in space and time. Journal of Applied Meteorology and Climatology, In press.

MacPherson, B., M. Lindskog, V. Durocq, M. Nuret, G. Gregoric, A. Rossa, G. Hasse, I. Holleman, and P. P. PAlberoni, 2003: Assimilation of radar data in Numerical Weather Predicition (NWP) models. Weather radar - Principles and advanced applications, P. Meishcner, Ed., Springer, 78-114.

Sheppard, B. E., 1990: Measurement of Raindrop Size Distributions Using a Small Doppler Radar. Journal of Atmospheric and Oceanic Technology, 7, 255-268.

Sun, J. and J. W. Wilson, 2003: The Assimilation of Radar Data for Weather Prediction. Meteorological Monographs 175-198.

Sun, J. Z., 2005: Convective-scale assimilation of radar data: Progress and challenges. Quarterly Journal of the Royal Meteorological Society, 131, 3439-3463.

Zawadzki, I., 1984: Factors affecting the precision of radar measurements of rain. Preprints, 22nd Int. Conf. on Radar Meteor., Zurich, Switzerland, Amer. Meteor. Soc., 251-256.